Selective attachment of benzonitrile on Si(111)-7×7: Configuration, selectivity, and mechanism

Feng Tao, Zhong Hai Wang, Xian Feng Chen, and Guo Qin Xu*
Department of Chemistry, National University of Singapore, 10 Kent Ridge, Singapore 119260
(Received 18 September 2001; published 21 February 2002)

The cycloaddition of benzonitrile with Si(111)-7×7 has been investigated as a model system for understanding the interaction of conjugated π-electron systems with Si(111)-7×7 using high-resolution electron energy loss spectroscopy, x-ray photoelectron spectroscopy (XPS), ultraviolet photoelectron spectroscopy, scanning-tunneling microscopy (STM), and density-functional-theory calculation (perturbative Beck-Perdew functional in conjugation with a basis set of DN**). Vibrational features of chemisorbed benzonitrile unambiguously demonstrate that the cyano group directly interacts with Si surface dangling bonds, evidenced in the disappearance of C≡N stretching mode around 2256 cm^{-1} coupled with the appearance of C=N stretching mode at 1623 cm^{-1} and the retention of all vibrational signatures of phenyl ring. XPS shows that both C 1*s* and N 1*s* core levels of the cyano groups display large down-shifts by 2.5 and 1.5 eV, respectively, after chemisorption. A smaller down-shift of ~0.8 eV is observed for the C 1*s* core level of phenyl group due to the weaker inductive effect of the formed C=N groups in chemisorbed benzonitrile than that of C≡N groups in physisorbed molecules. Compared with physisorbed molecules, the photoemission from π_{CN} orbitals of chemisorbed benzonitrile is significantly reduced, suggesting the direct involvement of π_{CN} in the surface binding. These experimental results show that the covalent attachment of benzonitrile on Si(111)-7×7 occurs in a selective manner through the (2+2) cycloaddition between the cyano group and the adjacent adatom-rest atom pair. The cycloadduct formed contains an intact phenyl ring protruding into vacuum, retaining aromaticity. This functionalized Si surface may serve as a substrate for further modification or act as an intermediate for fabrication of multilayer organic thin films or materials syntheses in vacuum.

DOI: 10.1103/PhysRevB.65.115311 PACS number(s): 68.43.Fg, 68.47.Pe

I. INTRODUCTION

There is growing interest in the modification of semiconductor surfaces with organic molecules[1] because the modified semiconductor surfaces are expected to have tailor-made electronic, optical, or biofunctional properties by adopting proper organic reactants with desired organic functionalities.[2,3] Another driving force to link organic molecules with semiconductor technology, as was well documented, is the expectation that this hybrid approach will possibly create new microelectronics and will enable the growth of multilayer organic thin films on semiconductor surfaces.[2,3] The present focus is to understand the reaction mechanisms of organic molecules on semiconductor surfaces. In particular, studies on the reactivity and selectivity of multifunctional organic molecules on semiconductor surfaces are quite important since one of the molecular functional groups can selectively bind on semiconductor surfaces and others are retained for further modification and materials syntheses in vacuum.

One of the most interesting semiconductor surfaces is Si(111)-7×7. Its surface structure was clearly demonstrated with the so-called dimer-adatom-stacking (DAS) faulted model,[4] as shown in Fig. 1. There are two subunits surrounded by nine Si dimers. The left subunit has a stacking fault. There are 19 dangling bonds associated with 12 adatoms, six rest-atoms, and one corner hole in a unit cell. Chemical reaction is most likely to take place at these dangling bonds. Previous work in this area mainly involves some unsaturated hydrocarbons containing unpolarized covalent bonds of C=C or C≡C, including typical ethylene,[5,6] acetylene,[7–9] five-membered heterocyclic aromatics,[10–13] benzene,[14,15] aniline,[16] and chlorobenzene.[17,18] These studies demonstrate that the adjacent adatom-rest atom pair can act as a ''diradical'' to react with unsaturated functional groups of organic molecules.

Especially, for benzene and its derivatives, the chemisorption mechanisms and binding configurations on silicon surfaces have been well demonstrated. Benzene adsorbs readily

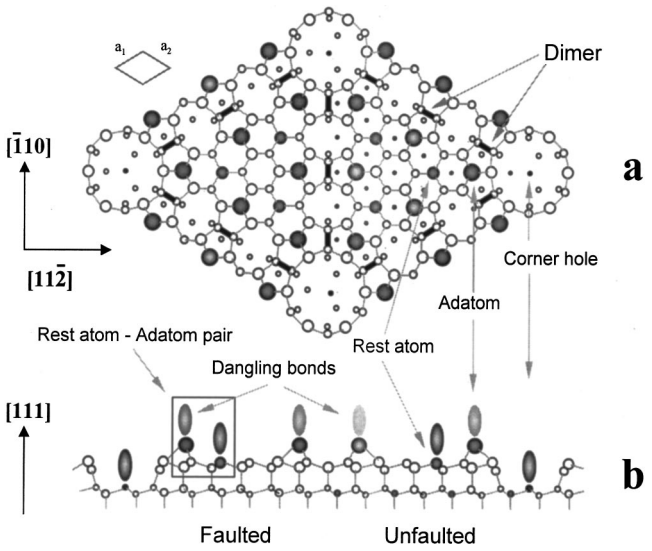

FIG. 1. Top (a) and side (b) views of the DAS model of Si(111)-7×7.

on Si(100) through a tetra-σ binding mode[14,19] and on Si(111)-7×7 via the typical (4+2) cycloaddition mechanism involving both 1,4-C atoms of benzene and the silicon surface dangling bonds.[15] Some benzene derivatives bind to silicon surfaces through a dissociated reaction pathway or/and molecular chemisorption via the direct participation of phenyl ring; for example, for toluene and xylene/Si(100),[20] IR results revealed the dissociated adsorption together with molecular chemisorption involving the cycloaddition of their 2,5-C atoms to the Si═Si dimer, indicating the loss of phenyl ring skeleton and aromaticity. For chlorobenzene on Si(111)-7×7,[17,18] high-resolution electron-energy-loss-spectroscopy (HREELS) results demonstrated the molecular chemisorption mechanism of a typical (4+2) cycloaddition involving 2,5-C atoms of chlorobenzene and adjacent adatom-rest atom pair.

Benzonitrile is an interesting multifunctional molecule due to its π-conjugated phenyl ring and cyano group. Its rich attachment chemistry on Si(111)-7×7 can be expected. It may selectively bind on Si(111)-7×7 through a typical (2+2) cycloaddition of the cyano group with an adjacent adatom-rest atom pair, maintaining its phenyl ring skeleton in the addition product. Another possibility is that it can bind to the surface through its phenyl ring in the binding modes similar to those of benzene and its derivatives.[14–18] Besides, the (4+2) cycloaddition between the C═C-C≡N group and neighboring adatom-rest atom pair is also possible. Thus, benzonitrile/Si(111)-7×7 was chosen as a model system to demonstrate the reactivity and selectivity of multifunctional molecules on Si(111)-7×7. In this work, we focus on the microscopic structure and binding mechanism of benzonitrile on Si(111)-7×7.

II. EXPERIMENT

The experiments were performed in three UHV chambers. All of them have a base pressure of less than 2×10^{-10} Torr, achieved with turbo-molecular and sputtered-ion pumps. The first UHV chamber was equipped with an x-ray gun (both Mg and Al anodes), He I and II UV source and hemispherical energy analyzer (CLAM 2, VG) for x-ray photoelectron spectroscopy (XPS) and ultraviolet photoelectron spectroscopy (UPS). The HREELS chamber mainly consists of a high-resolution electron energy loss spectrometer (HREELS, LK-2000-14*R*) and a quadruple mass spectrometer (UT1-100) for gas analysis. The scanning tunneling microscopy (STM) system includes a sample preparation chamber and the omicron VT STM chamber.

For HREELS experiments, the electron beam with an energy of 5.0 eV impinges on Si(111)-7×7 at an incident angle of 60° with a resolution of 5–6 meV [full width at half maximum (FWHM), 40–50 cm^{-1}]. XPS spectra were acquired using Al $K\alpha$ radiation ($h\nu=1486.6$ eV) and a 20 eV pass energy. For XPS, the binging energy (BE) scale is referenced to the peak maximum of the Si 2*p* line (99.3 eV) (Ref. 21) of a clean Si(111) substrate with a FWHM of less than 1.2 eV. He II ($h\nu=40.80$ eV) was selected to obtain valence band spectra for a wider energy window. In UPS studies, the pass energy was set at 10 eV. The constant current topographs (CCT's) of the clean and benzonitrile-exposed Si(111)-7×7 were usually obtained with a sample bias of $V_s=1-2$ V and a tunneling current of $I_t=0.15-0.2$ nA.

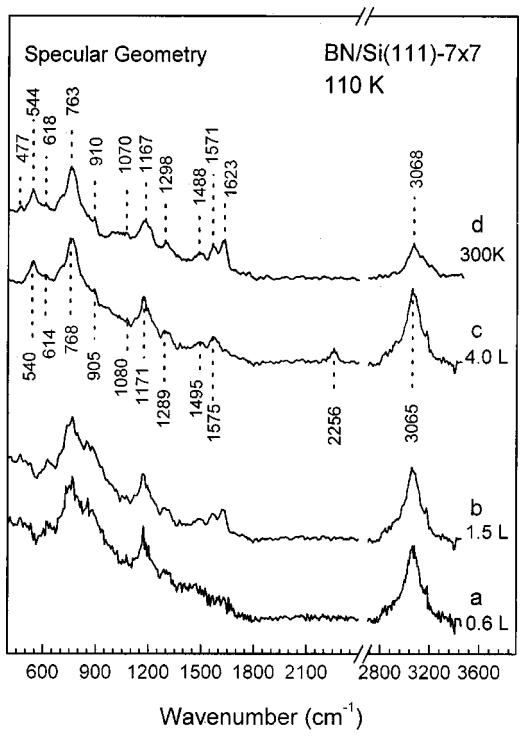

FIG. 2. HREEL spectra of benzonitrile on Si(111)-7×7 as a function of exposure at 110 K. $E_p=5.0$ eV, specular geometry.

For HREELS, XPS, and UPS experiments, the samples with a dimension of $8\times18\times0.35$ mm^3 ($3\times8\times0.35$ mm^3 for STM experiments) were cut from *p*-type Si(111) wafers (*B*-doped, with a resistivity of 1–30 Ω cm, Goodfellow); a Ta-sheet heater (0.025 mm thick) was sandwiched tightly between two Si(111) crystals held together by two Ta clips. Uniform heating of the samples was achieved by passing current through the Ta heater. This sample mounting configuration allows us to resistively heat the samples to 1400 K and conductively cool them to 110 K using liquid nitrogen. The temperature distribution on the samples is within ±10 K at 1000 K, determined using a pyrometer (TR-630, Minolta).

The Si(111) sample was cleaned by repeated ion sputtering-annealing cycles (500 eV Ar^+ bombardment for 30 min with an ion current density of 5–10 $\mu A\,cm^{-1}$ and subsequent annealing to 1250 K for 20 min). The surface cleanliness was routinely monitored using XPS, UPS, and HREELS. The (7×7) reconstruction was formed after the final annealing procedure. Benzonitrile (Aldrich, 99%) was purified by freeze-pump-thaw cycles and dosed onto Si(111)-7×7 by backfilling or direct dosing (for STM experiments) through a variable leaking valve without ion gauge sensitivity calibration.

III. RESULTS

A. High-resolution electron energy loss spectroscopy

Figures 2(a)–2(c) show the high-resolution electron en-

TABLE I. Vibrational frequencies of benzonitrile (BN) (cm^{-1}). sh means sharp; s means strong; m means medium; w means weak; vs means very strong.

Sys. Class	Description[a]	Liquid[a]	Physisorbed BN/Au(100)[b]	Chemisorbed BN/Au(100)[c]	Physisorbed BN/Si(111)-7×7[d]	Chemisorbed BN/Si(111)-7×7[d]
*b*2	ν(CH)	3087 (sh)				
*a*1	ν(CH)	3065 (s)	3080	3066	3065	3068
*a*1	ν(CH)	3042 (w)				
*b*2	ν(CH)	3030 (w)				
*a*1	ν(C≡N)	2229 (vs)	2247	(2234)	2256	
*a*1	ν(C═N)					1623
*a*1	ν(CC)	1598 (s)	1618		1575	1571
*b*2	ν(CC)	1580 (m)				
*a*1	ν(CC)	1492 (s)	1482[c]		1495	1488
*b*2	θ(CC)	1448 (s)	1482[c]			
*b*2	ν(CC)	1335 (m)				
*b*2	β(CH)	1287 (m)			1289	1298
*a*1	β(CH)	1179 (s)	1155[c]		1171	1167[c]
*b*2	β(CH)	1162 (m)				
*b*2	β(CH)	1071 (s)		1080	1070	
*a*1	β(CH)	1026 (s)	1002[c]			
*a*1	ν(C-CN)	1192 (s)	1155[c]			1167[c]
*a*1	Ring [*p*]	1000 (m)	1002[c]			
*b*1	γ(CH)	989 (w)				
*a*2	γ(CH)	975 (w)				
*b*1	γ(CH)	926 (s)	948		905	910
*a*2	γ(CH)	845 (m)				
*b*1	γ(CH)	758 (vs)	754	741	768	763
*a*1	ϕ(CC)	687 (vs)	Undersolved	Undersolved		
*a*2	ϕ(CC)	399 (vw)				
*b*2	α(CCC)	624 (w)			614	618
*a*1	ν(CC)	767 (w)				
*a*1	α(CCC)	461 (w)				
*b*1	ϕ(CC)	548 (vs)	588	545	540	544
	ν(SiC)					477
*b*2	β(CCN)	379 (m)	380			
*b*1	γ(CCN)	172 (s)	180			
*b*2	β(CN)	549 (w)				
*b*1	γ(CN)	157 (sh)				

[a]Reference 22.
[b]Reference 23.
[c]Frequency used again.
[d]This work.

ergy loss spectra obtained after benzonitrile adsorption on Si(111)-7×7 at 110 K. Figure 2(d) shows the vibrational features of chemisorbed benzonitrile/Si(111)-7×7 after annealing the multilayer benzonitrile-covered silicon sample to 300 K to desorb physisorbed molecules. The vibrational frequencies and corresponding assignments for physisorbed [Fig. 2(c)] and chemisorbed benzonitrile [Fig. 2(d)] are listed in Table I. From Table I, it can be seen that all vibrational features of physisorbed benzonitrile agree well with the infrared analyses of liquid phase benzonitrile[22] and previous infrared studies of physisorbed benzonitrile on Au(100).[23]

However, the features of chemisorbed benzonitrile [Figs. 2(a), 2(b), and 2(d)] are significantly different from the above-mentioned physisorbed molecules [Fig. 2(c)]. The $\nu_{C\equiv N}$ stretching mode at 2256 cm^{-1} observed for physisorbed benzonitrile is not present in the spectra of chemisorbed molecules. The new feature at 1623 cm^{-1} clearly resolved for chemisorbed benzonitrile [Figs. 2(b) and 2(d)] can be assigned to the stretching mode of the C═N bond though its loss intensity is weak possibly due to the nearly parallel configuration.[24] The absence of $\nu_{C\equiv N}$ coupled with the concurrent emergence of $\nu_{C=N}$ in the HREELS of chemisorbed

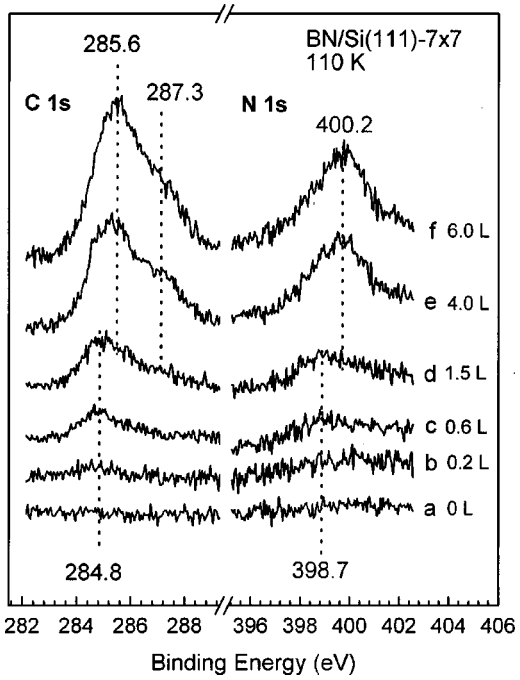

FIG. 3. C 1*s* and N 1*s* spectra of benzonitrile on Si(111)-7×7 as a function of exposure at 110 K.

benzonitrile strongly supports that the cyano group directly participates in the covalent binding with Si(111)-7×7. In addition, the identical vibrational feature for C—H stretching mode was observed for both the chemisorbed (at 3065 cm^{-1}) and physisorbed (at 3068 cm^{-1}) benzonitrile, indicating the retention of sp^2 hybridization for the carbon atoms of phenyl ring. Furthermore, the characteristic vibrational modes of monosubstituted benzene,[25] γ(C—H) around 750 cm^{-1} and ν(C—C) around 1560–1615 cm^{-1} and 1450–1525 cm^{-1} are also retained in the HREELS spectra of chemisorbed benzonitrile. These results suggest that the phenyl ring does not directly interact with Si(111)-7×7, maintaining the phenyl ring skeleton and aromaticity in the chemisorbed benzonitrile.

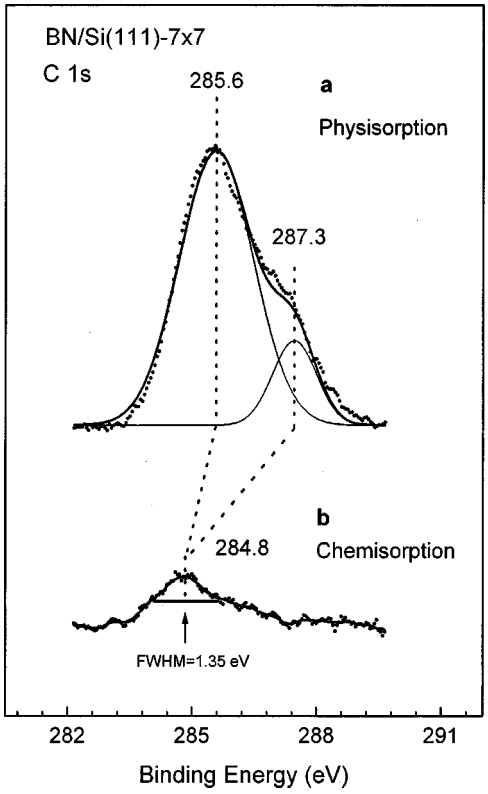

FIG. 4. The deconvoluted C 1*s* spectra of physisorbed and chemisorbed benzonitrile on Si(111)-7×7.

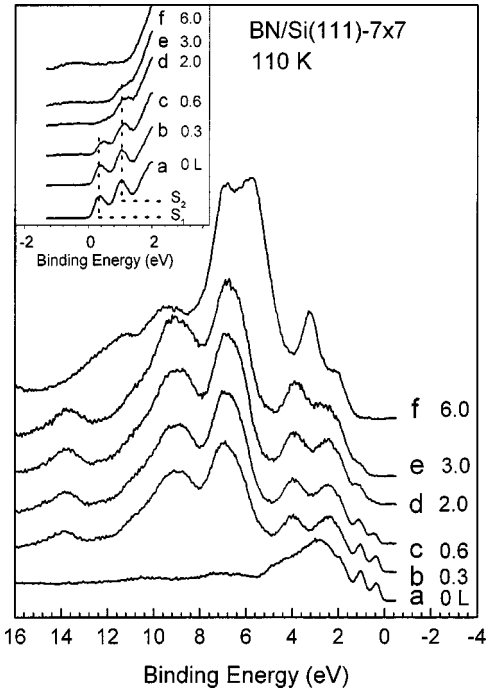

FIG. 5. UPS spectra for benzonitrile on Si(111)-7×7 as a function of exposure at 110 K.

B. X-ray photoelectron spectroscopy

XPS was employed to investigate the chemical shifts of C 1*s* and N 1*s* core levels of benzonitrile on Si(111)-7×7. The C 1*s* and N 1*s* spectra of benzonitrile following a sequence of exposures at 110 K are shown in Fig. 3. The broad sloping background present in the N 1*s* spectra is possibly due to the photoemission from the Ta $4p_{3/2}$ level of the crystal's mounting.[26] For benzonitrile exposures $\leqslant$1.5 L, a C 1*s* peak at 284.8 eV and a N 1*s* peak at 398.7 eV were observed, attributed to chemisorbed benzonitrile. With increasing exposure, new photoemission features on the higher BE sides of the C 1*s* and N 1*s* peaks of chemisorbed benzonitrile grow preferentially. Meanwhile, the features of chemisorbed benzonitrile are significantly attenuated. At high exposures, an obvious asymmetric peak for C 1*s* at ~285.6 eV with a shoulder at ~287.3 eV and a peak for N 1*s* at 400.2 eV become dominant due to physisorbed benzonitrile. In order to assign C 1*s* peaks of physisorbed and chemisorbed benzonitrile, software VGX900 (VG) was commanded to deconvolute the XPS spectra. The fitting results are presented in Fig. 4. Figure 4(a) shows that the C 1*s* peak for phys-

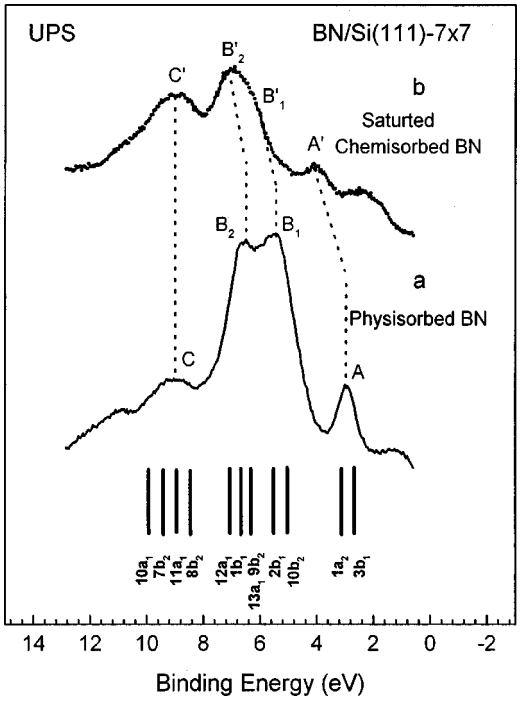

FIG. 6. Valence band spectrum of physisorbed benzonitrile (a) and difference spectrum of saturated chemisorbed molecules on Si(111)-7×7 obtained by subtracting the photoemission of a clean Si(111)-7×7 surface from that of a fully chemisorbed benzonitrile/Si(111)-7×7 (b). The bar graph below Fig. 6(a) is the orbital energy level of gaseous benzonitrile, shifted to account for work function and final-state relaxation effects when condensed on solid-state surfaces.

isorbed benzonitrile can be reasonably deconvoluted into two peaks at 287.3 and 285.6 eV with an area ratio of 1:5.6, assigned to the cyano and phenyl ring, respectively. The FWHM (1.65 eV) of the peak at 285.6 eV is larger than that (1.25 eV) of the peak at 287.3 eV, indicating the uneven distribution of electron density on phenyl ring due to the strong inductive effect of the cyano group. However, the C 1*s* spectrum of the chemisorbed benzonitrile [Fig. 4(b)] is quite different. Its FWHM of 1.35 eV and nearly symmetrical peak shape suggest the unresolvable nature of the inequivalent carbon atoms in the chemisorbed benzonitrile.

C. Ultraviolet photoelectron spectroscopy

Valence band spectra of adsorbed benzonitrile on Si(111)-7×7 at 110 K as a function of the expsoure are shown in Fig. 5. For the clean Si(111)-7×7 surface, the two peaks at ~0.3 (S_1) and ~1.0 eV (S_2) below E_F (the inset of Fig. 5) are due to the dangling bond surface states of adatoms and rest atoms, respectively, according to the STM studies.[27,28] Increasing benzonitrile exposure leads to the gradual attenuation of these states (the inset of Fig. 5), possibly caused by the redistribution of their electron density in the resulting adsorbate-substrate complex.

For Figs. 5(b)–5(e), chemisorbed-species-induced emissions appear with maxima at ~2.6, 4.1, 7.2, 9.1, and 13.8 eV below E_F. With increasing exposure, benzonitrile multilayer grows up and the features of the chemisorbed layer are attenuated. In order to demonstrate the contribution of orbitals in the interaction of benzonitrile with Si(111)-7×7, both the physisorbed multilayer spectrum and the difference spectrum of chemisorbed monolayer are presented in Fig. 6. The saturated chemisorption monolayer was fabicated by annealing the benzonitrile-exposed Si(111)-7×7 to 300 K to drive away all the physisorbed multilayer and maintain only the chemisorbed molecules on the surface. The difference spectrum [Fig. 6(b)] was obtained by substracting the photoemission signals of a clean surface from those of a fully chemisorbed benzonitrile/Si(111)-7×7. The orbital energy levels of gaseous benzonitrile[29] are shown in the form of bar graph below Fig. 6(a), shifted to account for work function and final-state relaxation effects when condensed on solid-state surfaces. The close resemblance of the valence band spectrum at 6.0 L benzonitrile exposure on Si(111)-7×7 at 110 K with the gas phase spectrum,[29] clearly demonstrates the formation of benzonitrile multilayer. In the UPS of physisorbed multilayer [Fig. 6(a)], the peak *A* at 3.4 eV is assigned to the convolution of the $3b_1$ and $1a_2$ levels of the π characters of intact benzonitrile. In addition, a broadband (*B*) extending from 4.0 to 8.0 eV consists of emissions from five overlapping levels, including $\pi_{O\equiv N}$ of in-plane ($10b_2$) and out-of-plane ($2b_1$), *B*(19) ($9b_2$), *B*(18) ($13a_1$), π_1 ($1b_1$), and $\sigma_{C\equiv N}$($12a_1$). In Band *B* of Fig. 6(a), Peak B_1 is mainly contributed from the photoemission of two π_{CN} orbitals. Compared to physisorbed benzonitrile [Fig. 6(a)], the relative contribution (Peak B_1) from the photoemission of π_{CN} is significantly weakened in the difference spectrum of chemisorbed benzonitrile monolayer [Fig. 6(b)]. The reduction of photoemission from π_{CN} also strongly suggests that the cyano group directly interacts with Si surface dangling bonds.

D. Scanning-tunneling microscopy

In order to further elucidate the nature of benzonitrile chemisorbed on Si(111)-7×7, STM was used to investigate the extent and spatial distribution of the present surface reaction system at atomic resolution. The STM CCT's taken with +1.5 V sample bias and 300 K sample temperature are shown in Fig. 7. The adatoms, the corner holes, and the dimer boundaries can be clearly seen in the image of a clean Si(111)-7×7 surface [Fig. 7(a)]. The density of adatom defects is found to be low on our routinely obtained clean surfaces. By counting more than 1500 adatoms, the defect density was estimated to be less than 1%.

Figure 7(b) is the typical STM topograph of Si(111)-7×7 exposed to benzonitrile of 0.1 L (direct dosing) at room temperature. Comparison with the clean surface reveals that the 7×7 reconstruction is preserved after benzonitrile adsorption reaction. However, some surface adatoms become invisible as a result of the reaction, increasing in number with the benzonitrile exposure. The apparent formation of darkened sites was also observed in the adsorption of other small molecules, such as, NH_3,[28] H_2O,[30] C_2H_2,[8] C_2H_4,[31] C_6H_6,[32] C_6H_5Cl,[8] and C_4H_5S[12] on Si(111)-7×7. In all these cases, the darkness of the adatoms in the STM images was attributed to the consumption of the adatom dangling

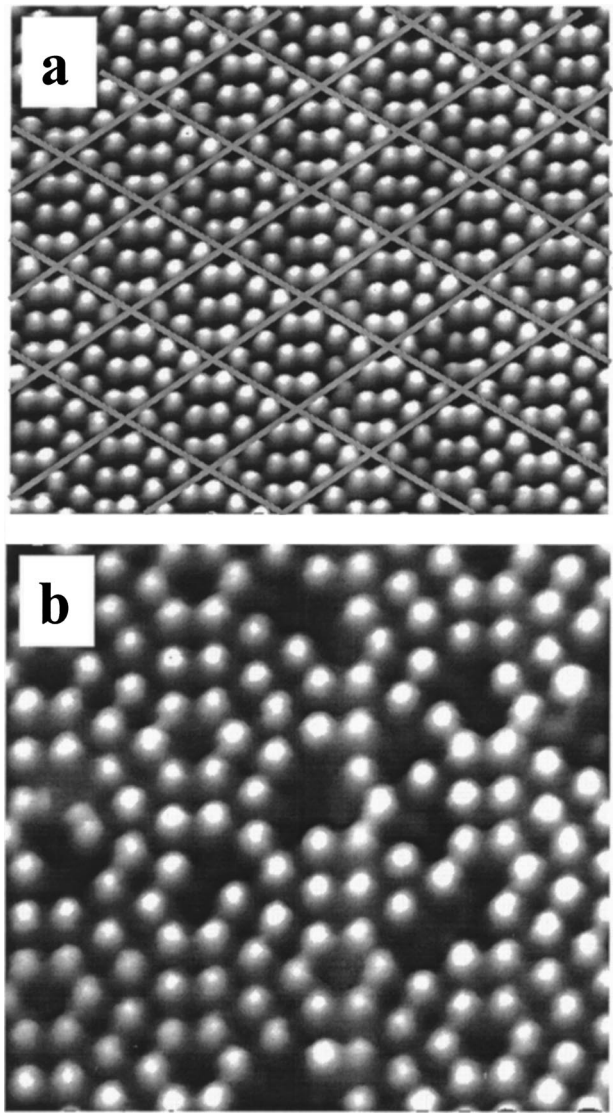

FIG. 7. Constant-current-topograph (CCT) images of clean (a) and benzonitrile-exposed (b) Si(111)-7×7.

bonds due to the surface adsorbates bond formation. We found no bias dependence for the intensity at the reacted adatoms (darkened sites), suggesting that the adsorbed benzonitrile and reacted adatoms do not have orbitals close to the Fermi energy E_F, consistent with the consumption of surface dangling bonds observed in UPS studies (Fig. 5).

The statistical counting of darkened dangling bond sites can provide the information regarding the spatial selectivity for the covalent attachment of benzonitrile on Si(111)-7×7. On a surface exposed to 0.4 L (direct dosing), the statistical counting on 80 unit cells reveals that there are ~180 center adatoms and ~72 corner adatoms among the ~252 darkened adatoms. In addition, ~163 of the total reacted adatoms are located in the faulted subunits while ~89 in the unfaulted subunits. Similar results were obtained after close examination of several different regions on the same sample. The reactivity of center adatoms is about twice that of the corner adatoms and the adatoms in faulted subunits react preferentially over those in unfaulted subunits with a ratio of

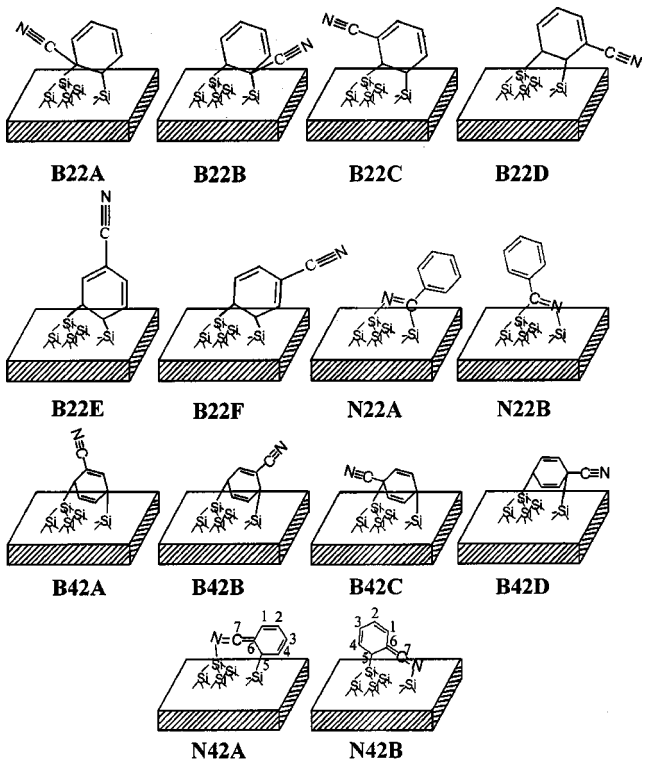

FIG. 8. Scheme of possible binding modes of benzonitrile on Si(111)-7×7.

1.8. It is noted that intrinsic vacancy defects may be included in the accounting. However, its number is not significant, i.e., less than 1%. The preferential binding of benzonitrile with the adatom sites on the faulted halves of the Si(111)-7×7 unit cells can be understood considering the higher electrophilicity of the faulted subunits.[31] On the other hand, the DAS (7×7) model (Fig. 1) shows that the reaction at a corner adatom may strain two dimer bonds, while it will strain only one for the center adatom. Thus, a smaller strain induced by the chemisorbed benzonitrile at a center adatom site would possibly result in a lower energy of the transition state, leading to a higher reactivity at the center adatom sites.[32–34]

E. Density-functional-theory (DFT) calculation

Benzonitrile contains two potentially reactive function groups, namely, the phenyl ring and cyano group. These two groups can react with the surface on their own or cooperatively. As a result, a number of adsorption configurations are possible if only the di-σ binding is considered for the chemisorption process. There are 14 possible binding configurations for benzonitrile molecularly chemisorbed on Si(111)-7×7, including the (2+2) and (4+2) attachments (Fig. 8). The direct interactions between carbon atoms of phenyl ring and adjacent adatom-rest atom pair are presented in Models *B22A*, *B22B*, *B22C*, *B22D*, *B22E*, *B22F*, *B42A*, *B42B*, *B42C*, and *B42D*. In addition, there are other two possibilities involving the direct participation of the cyano group, including the (4+2) cycloaddition via the C═C-C≡N group (models *N42A* and *N42B*) and the (2+2) cycloaddition

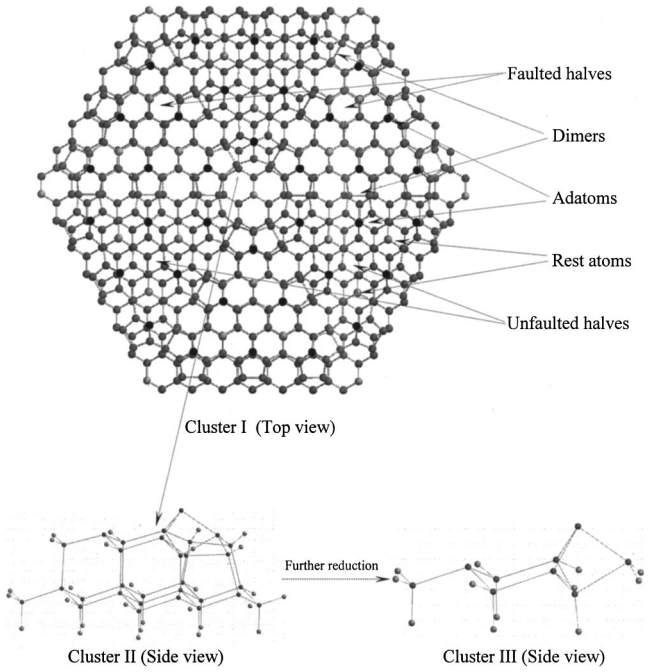

FIG. 9. A large cluster of the top five silicon layers constructed based on the DAS model to present three Si(111)-7×7 surface unit cells surrounding a corner hole. It (cluster I) has 973 atoms including the capping H atoms (not displayed for clarity). Cluster II ($Si_{30}H_{28}$) and III (Si_9H_{12}) are reduced from Cluster I.

through the cyano group (models *N*22*A* and *N*22*B*). Our DFT modeling focuses on the geometry optimization and the calculation of the formation heat for all these possible binding models to gain a better understanding on the molecular chemisorption of benzonitrile.

As shown in the left bottom panel of Fig. 9, cluster II ($Si_{30}H_{28}$) was cut from the central part of *MMFF*94[35] optimized cluster I containing 973 atoms including the capping H atoms (the top panel of Fig. 9), where the precision of atomic positions suffers the least from boundary effects. It contains an adatom and a neighboring rest atom from an unfaulted subunit, serving as a "di-σ" binding site for the attachment of one benzonitrile molecule. Capping H atoms at the cluster boundaries are kept frozen. Silicon atoms in the bottom double layer are placed at bulk lattice positions prior to the geometry optimization process, with each Si—Si bond length set to 2.3517 Å and all bond angles adjusted to 109.4712°. Cluster III (Si_9H_{12}) was obtained from further reduction of cluster II. Similarly, all capping H atoms were frozen during geometry optimization. Fourteen clusters (not shown) corresponding to the possible binding models shown in Fig. 8 were constructed by addition of C_6H_5CN onto the mother cluster (cluster III of Fig. 9). Clusters I, II, and III were constructed by us and successfully predicted the adsorption energy of benzene on Si(111)-7×7.[15,36]

Calculations were performed using SPARTAN package.[37] The heat of adsorption of 14 binding configurations was calculated at the DFT theory level using perturbative Beck-Perdew functional (pBP86) in conjugation with a basis set of DN** (comparable 6-31 *G***).[36] Geometric optimizations were conducted under SPARTAN default criteria. Heat of formation listed in Table II, synonymous to adsorption energy, is quoted here as the difference between the energy of the adsorbate /substrate complex and the total sum of the substrate and gaseous molecule.

Table II shows that the *N*22*B* is most stable, where the C and N atoms in the CN functional group bond to the adatom and rest atom, respectively. The phenyl ring remains intact in this configuration, pointing away from the surface without much steric interaction. The resulting C═N group stays conjugated to the phenyl ring. Such conjugation effect is maximized due to their co-planar arrangement, possibly compensating the inevitable strain caused by the mismatch between the dimension of the C═N and the adatom-rest atom distance.

The configuration closest in energy to *N*22*B*, besides *N*22*A*, is the *N*42*B*, where both the phenyl ring and the CN group participate in the adsorption. Although losing the aromaticity of the system, it yet suffers much less steric strain compared to the (2+2) cycloadduct, resulting in a similar stability to the *N*22*B* configuration. The (4+2) cycloaddition with only phenyl ring (Models *B*42*A*, *B*42*B*, *B*42*C* and *B*42*D*) participating in adsorption are slightly less stable.

Based on these thermodynamic data, a selectivity of 7:3 ratio or higher between the *N*22*B* and other models can be established, assuming Boltzman distribution at a temperature of 298 K. However, when these chemisorption states are not easily interconvertible, it may be the kinetic factor that dominantly determines the selectivity among various configurations. Our experimental observation of the CN group involved in the binding and the retention of phenyl ring excludes the two possible (4+2) cycloadditions (models *N*42*A* and *N*42*B*).

IV. DISCUSSION

Taguchi *et al.*[19] found that the C-H stretching mode presents two isolated peaks at 3065 [(sp^2)C-H] and 2935 [(sp^3)C-H] cm^{-1} in chemisorbed benzene on Si(100) due to the rehybridization of a portion of carbon atoms of benzene from sp^2 to sp^3. For chemisorbed benzene on Si(111)-7×7, we also observed two well-resolved C—H stretching peaks due to the co-existence of C(sp^2)-H and C(sp^3)-H.[15] However, our HREELS measurements of

TABLE II. The heat of formation of modes corresponding to (2+2) and (4+2) cycloadditions. Energies are in kcal mol^{-1}.

	*B*22*A*	*B*22*B*	*B*22*C*	*B*22*D*	*B*22*E*	*B*22*F*	*N*22*A*	*N*22*B*	*B*42*A*	*B*42*B*	*B*42*C*	*B*42*D*	*N*42*A*	*N*42*B*
Heat of formation	+6.4	+9.3	+3.5	+4.2	+5.3	+6.7	−27.1	−28.9	−26.3	−21.5	−26.4	−20.8	−23.2	−26.9

chemisorbed benzonitrile show that all the vibrational modes related to C—H remain unchanged. Particularly, the C—H stretching mode still appears as a single peak around 3065 cm^{-1}, similar to the case of physisorbed benzonitrile (Fig. 2). This observation together with the absence of the stretching mode of C≡N and appearance of the C═N vibration unambiguously excludes the possible binding modes only involving the carbon atoms of phenyl ring (modes *B*22*A*, *B*22*B*, *B*22*C*, *B*22*D*, *B*22*E*, *B*22*F*, *B*42*A*, *B*42*B*, *B*42*C* and *B*42*D*). In fact, the absence of rehybridization in the C atoms of phenyl ring evidenced from the retention of C(sp^2)-H vibrational features also rules out the possibility of *N*42*A* and *N*42*B*. Hence, the vibrational features of chemisorbed benzonitrile conclusively demonstrate that benzonitrile selectively bonds to Si(111)-7×7 through the interaction between one π bond of the cyano group and a adjacent adatom-rest atom pair via the (2+2) cycloaddition. Although the DFT calculation predicts the adsorption energy of (4+2) cycloaddition (model *B*42*A*, *B*42*B*, *B*42*C*, *B*42*D*, *N*42*A*, and *N*42*B* in Table II) is similar to that of (2+2) cycloaddition occuring at cyano group (*N*22*A* and *N*22*B*), no experimental evidence supports them, possibly attributable to the higher energy of transition state resulted from breaking the conjugation π electronic structure of phenyl ring and losing its aromacity.

XPS results show that both C 1*s* and N 1*s* core levels of the cyano group display large chemical shifts upon benzonitrile chemisorption on Si(111)-7×7. The C 1*s* and N 1*s* spectra shown in Fig. 4(b) can be reasonably explained by the (2+2) cycloaddition occuring at the cyano group. When the C≡N group reacts with Si surface dangling bonds, both C 1*s* and N 1*s* core-levels of the cyano are shifted by −2.5 and −1.5 eV, respectively, similar to those observed for the di-σ bonded acetonitrile on Ni(111).[38] Besides, the C 1*s* core level of the six C atoms of phenyl ring also displays a downshift of 0.8 eV upon chemisorption, attributable to the weaker inductive effect of the (Si)C═N(Si) group in chemisorbed benzonitrile than that of the C≡N group in physisorbed molecules. The nearly symmetrical peak-shape and narrow FWHM of the C 1*s* peak of chemisorbed benzonitrile imply that seven C atoms of chemisorbed benzonitrile have a similar binding energy of 284.8 eV, possibly due to the combined inductive and conjugation effects between phenyl ring and the formed C═N group. Our UPS also reveals that π_{CN} directly participates in the interaction with Si surface, well consistent with the HREELS and XPS results.

V. SUMMARY

Benzonitrile interacts with Si(111)-7×7 in a selective covalent binding of the cyano group to a neighboring adatom-rest atom pair via a (2+2) cycloaddition mechanism. The unreacted phenyl ring may serve as a platform for attaching other molecules to fabricate Si-based organic thin films and develop potential Si-based microelectronic devices or as an intermediate in further reaction with chosen organic functionalities for materials synthesis under vacuum condition through typical phenyl ring reactions.[39,40]

*Corresponding author. FAX: (65) 779 1691, Email address: chmxugq@nus.edu.sg

[1] J. T. Yates, Jr., Science **279**, 335 (1998).
[2] R. J. Hamers, S. K. Coulter, M. D. Ellison, J. S. Hovis, D. F. Padowitz, M. P. Schwartz, C. M. Greenlief, and J. N. Russell, Jr., Acc. Chem. Res. **33**, 617 (2000).
[3] R. A. Wolkow, Annu. Rev. Phys. Chem. **50**, 413 (1999).
[4] D. J. Chadi, Phys. Rev. Lett. **43**, 43 (1979).
[5] F. Rochet, F. Jolly, G. Dufour, F. Sirotti, and J. L. Cantin, Phys. Rev. B **58**, 11 029 (1998).
[6] M. Carbone, M. Zanoni, M. N. Piancastelli, G. Comtet, G. Dujardin, L. Hellner, and A. Mayner, J. Electron Spectrosc. Relat. Phenom. **76**, 271 (1995).
[7] F. Rochet, G. Dufour, P. Prieto, F. Sirotti, and F. C. Stedile, Phys. Rev. B **57**, 6738 (1998).
[8] J. Yoshinobu, D. Fukushi, M. Uda, E. Nomura, and M. Aono, Phys. Rev. B **46**, 9520 (1992).
[9] B. Weiner, C. S. Carmer, and M. Frenklach, Phys. Rev. B **43**, 1678 (1991).
[10] Y. Cao, Z. H. Wang, J. F. Deng, and G. Q. Xu, Angew. Chem. Int. Edit. **39**, 2740 (2000).
[11] S. Letarte, A. Adnot, and D. Roy, Surf. Sci. **448**, 212 (2000).
[12] Y. Cao, K. S. Yong, Z. Q. Wang, W. S. Chin, Y. H. Lai, S. F. Deng, and G. Q. Xu, J. Am. Chem. Soc. **122**, 1812 (2000).
[13] C. D. Macpherson and K. T. Leung, Phys. Rev. B **51**, 17 995 (1995).
[14] M. Carbone, M. N. Piancastelli, M. P. Casaletto, R. Zanoni, G. Comtet, G. Dujardin, and J. L. Hellner, Phys. Rev. B **61**, 8531 (2000).
[15] Y. Cao, X. M. Wei, W. S. Chin, Y. H. Lai, J. F. Deng, S. L. Bernasek, and G. Q. Xu, J. Phys. Chem. B **103**, 5698 (1999).
[16] H. Tomimoto, R. Sumii, N. Shirota, S. Yagi, M. Taniguchi, T. Sekitani, and K. Tanaka, J. Vac. Sci. Technol. B **18**, 2335 (2000).
[17] Y. Cao, J. F. Deng, and G. Q. Xu, J. Chem. Phys. **112**, 4759 (2000).
[18] X. H. Chen, Q. Kong, J. C. Polanyi, D. Rogers, and S. So, Surf. Sci. **340**, 224 (1995).
[19] Y. Taguchi, M. Fujisawa, T. Takaoka, Y. Okada, and M. Nishijima, J. Chem. Phys. **95**, 6870 (1991).
[20] S. K. Coulter, J. S. Hovis, M. D. Ellison, and R. J. Hamers, J. Vac. Sci. Technol. A **18**, 1965 (2000).
[21] J. F. Moulder, W. F. Stickle, P. E. Sobol, and K. D. Bomben, *Handbook of x-ray Photoelectron Spectroscopy* (Physical Electronics Division, Perkin-Elmer Corporation, Minnesota, 1991).
[22] J. H. Green and D. J. Harrison, Spectrochim. Acta, Part A **32**, 1297 (1975).
[23] T. Solomun, K. Christmann, and H. Baumgartell, J. Phys. Chem. **93**, 7199 (1989).
[24] H. Ibach and D. L. Mills, *Electron Energy Loss Spectroscopy and Surface Vibrations* (Academic, New York, 1982).
[25] L. V. Daimay, B. C. Norman, G. F. William, and G. G. Jeanette, *The Handbook of Infrared and Raman Characteristic Frequencies of Organic Molecules* (Academic, Boston, 1991).
[26] M. R. Cohen, R. P. Merrill, Surf. Sci. **245**, 1 (1991).

[27] R. J. Hamers, Ph. Avouris, F. Bozso, Phys. Rev. Lett. **59**, 2071 (1987).
[28] Ph. Avouris, R. A. Wolkow, Phys. Rev. B **39**, 5091 (1989).
[29] K. Kimura, S. Katsumata, Y. Achiba, T. Yamazaki, and S. Itawa, *Handbook of He I Photoelectron Spectra of Fundamental Organic Molecules* (Japan Scientific Societies, Tokyo, 1981).
[30] Ph. Avouris and I. W. Lyo, Surf. Sci. **242**, 1 (1991).
[31] J. Yoshinobu, T. Tasuda, M. Onchi, and M. Nishijima, Chem. Phys. Lett. **130**, 170 (1986).
[32] R. A. Wolkow, D. J. Moffatt, J. Chem. Phys. **103**, 10 696 (1995).
[33] K. D. Brommer, M. Galvan, A. Dal Pino, Jr., and J. D. Joannopoulos, Surf. Sci. **314**, 57 (1994).
[34] R. A. Wolkow and Ph. Avouris, Phys. Rev. Lett. **60**, 1049 (1988).
[35] T. A. Halgren, J. Comput. Chem. **17**, 490 (1996).
[36] Z. H. Wang, Y. Cao, and G. Q. Xu, Chem. Phys. Lett. **338**, 7 (2001).
[37] W. J. Hehre, J. Yu, P. E. Klunzinger, and L. Lou, *A Brief Guide to Molecular Mechanics and Quantum Chemical Calculation* (Wavefunction, Irvine, CA, 1998).
[38] K. Kishi and S. Ikeda, Surf. Sci. **107**, 405 (1981).
[39] L. G. Wade, Jr. *Organic Chemistry*, 3rd ed. (Prentice-Hall, Englewood Cliffs, New Jersey, 1995).
[40] R. T. Morrison and R. N. Boyd, *Organic Chemistry* (Allyn and Bacon, Boston, 1959).